Supporting Information

n-Butanol/Water Interface Aided Physico-Chemical Tuning of Two-Dimensional Transition Metal Oxides

Rasha Rahman Poolakkandy[†], Subin Kaladi Chondath[†], Nesleena Puthiyottil[†], Dayana Davis[‡], and Mini Mol Menamparambath[†,]*

[†] Department of Chemistry, National Institute of Technology Calicut, NIT Campus PO, Chathamangalam, Calicut Dt., 673601, Kerala, India

[‡] Department of Chemistry, St. Joseph's College, Irinjalakuda PO, Thrissur Dt., 680121, Kerala, India

*Email : *minimol@nitc.ac.in, neeharabindu@gmail.com*

Chemicals and reagents

Nickel (II) chloride (Alfa Aesar, B22085, 98%), cobalt (II) chloride (Fisher Scientific, 22643, 97%), urea (Fisher Scientific, 20885, 99%), n-butanol (Fisher Scientific, 71-36-3), dopamine hydrochloride (Sigma-Aldrich, 62-31-7, 98%), L-ascorbic acid (Sigma-Aldrich, 50-81-7, 99%), uric acid (Alfa Aesar, A13346, 99%), nafion D-520 dispersion (Alfa Aesar, 42118) and ethanol (Changshu Hongsheng Fine Chemical Co. Ltd., Analytical reagent grade) were used as procured. Deionized (DI) water (> 18 MΩ) was used all through the synthesis. 0.1 molar phosphate buffer solution of pH 7.2 was used for the electrochemical studies.

Sl No	Volume of Solvent		Solvent Volume Ratio (Butanol:Water)	Sample Code
	Butanol (ml)	Water (ml)		
1	0	75	0:1	SS 1
2	25	50	1:2	BS 1
3	30	45	1:1.5	BS 2
4	37.5	37.5	1:1	BS 3
5	45	30	1.5:1	BS 4
6	50	25	2:1	BS 5
7	75	0	1:0	SS 2

Table S1. The solvent volume ratio of n-butanol and water used for the synthesis of the samples and the corresponding sample codes.

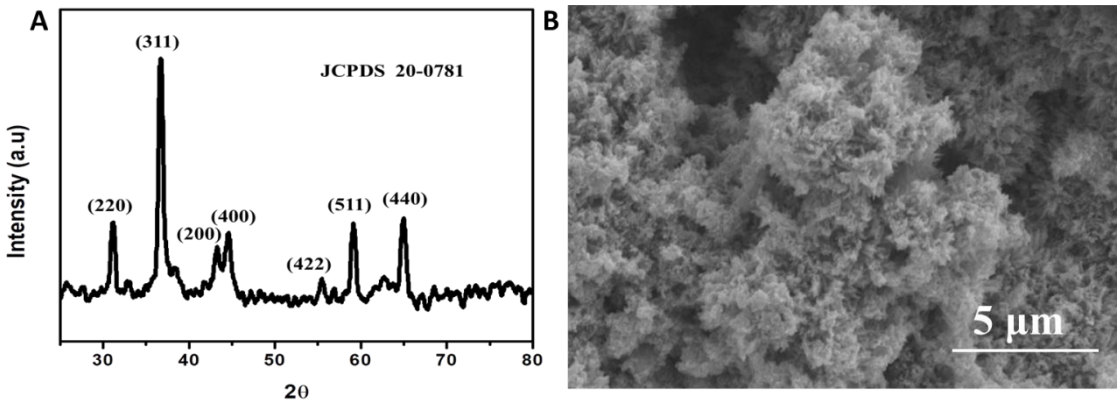

Figure S1. The XRD spectra (**A**) and the corresponding SEM image (**B**) of SS 1 annealed at 500℃.

The peaks with 2θ values 31.2°, 36.6°, 44.8°, 55.5°, 59.02° and 65° correspond to the planes (220), (311), (400), (422), (511) and (440) of nickel cobaltite (JCPDS 20-0781).[1] The peak at 43.28° corresponds to the (200) plane of NiO, which may be present in the system as a byproduct of annealing.[2]

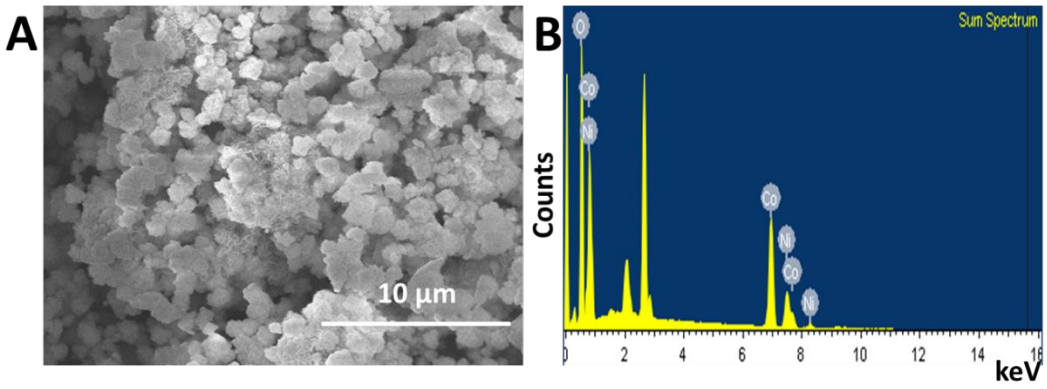

Figure S2. The SEM image corresponding to the EDAX analysis (A) and the corresponding spectra (B) for BS 3.

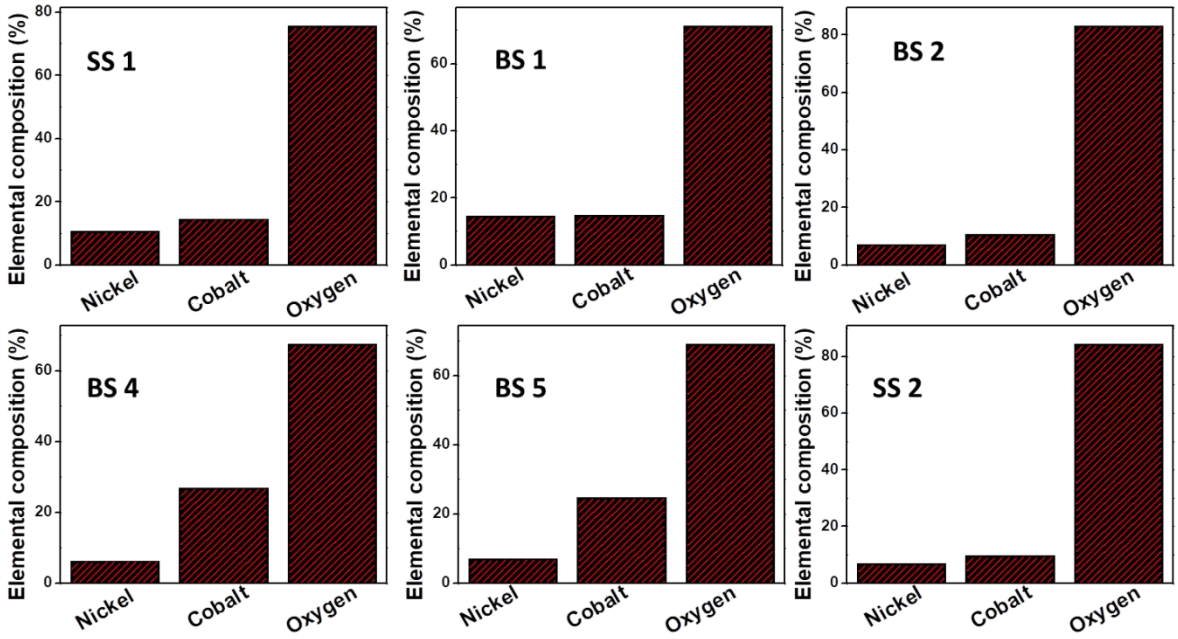

Figure S3. Elemental composition of the samples at varying solvent ratio.

The samples SS 1, SS2, BS 1 and BS 2 contain almost equal amount of nickel and cobalt, whereas BS 4 and BS 5 contain more amount of cobalt, which is in accordance with the colour in the optical images.

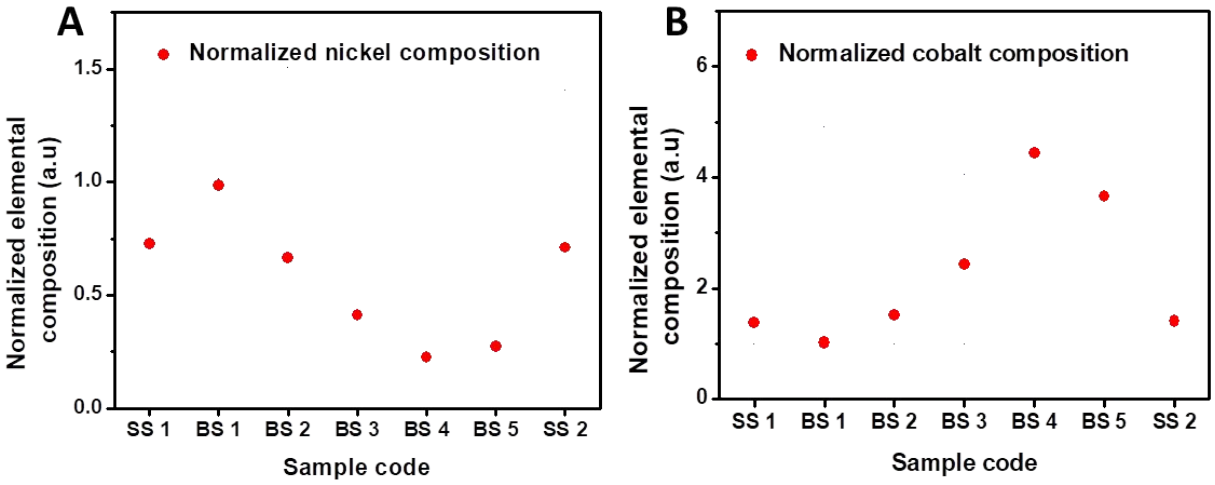

Figure S4. Normalized composition of nickel and cobalt atoms of samples SS 1, BS 1, BS 2, BS 3, BS 4, BS 5 and SS 2. (A) Nickel normalized to cobalt atoms and (B) cobalt normalized to nickel atoms.

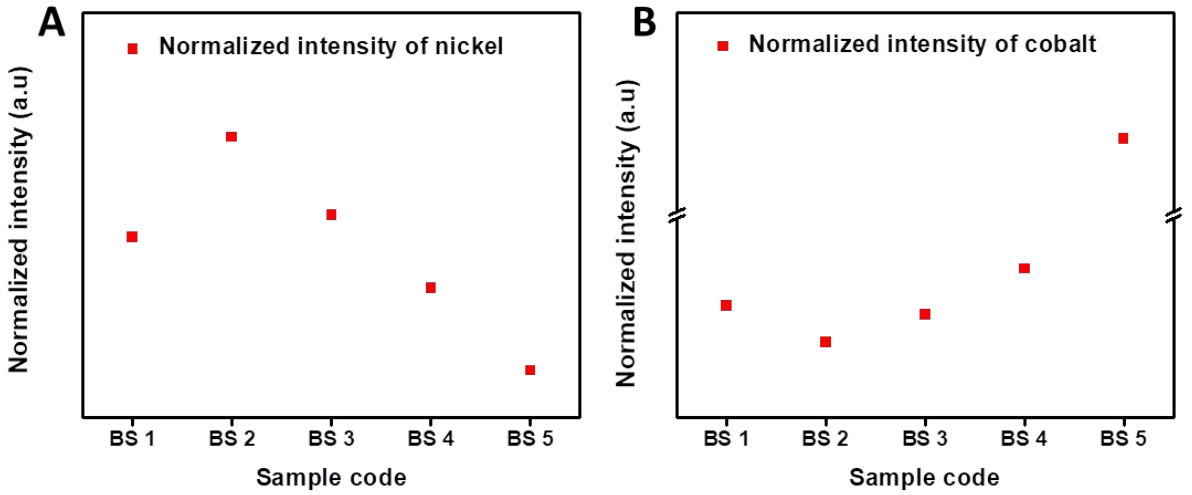

Figure S5. Normalized UV-Visible intensities of the samples SS 1, BS 1, BS 2, BS 3, BS 4, BS 5 and SS 2. (A) Nickel normalized to cobalt intensity and (B) cobalt normalized to nickel intensity.

The extraction of metal ions with the help of complexing agent urea at the n-butanol – water interface is investigated using UV-VIS spectroscopy. The concentrations of Ni and Co metal salts in water and complexing agent urea in n-butanol is maintained as per the reaction conditions of BS 1 to BS 5. The mixture is kept stirring for 2 hours at 70 ºC and the aqueous layer is analyzed for the concentrations of metal ions before and after stirring as shown in Figure S5. The composition of nickel is higher in the

samples BS 1 and BS 2, which are in the smaller ratios of n-butanol/water. However, the composition of cobalt is more in the samples BS 3, BS 4, and BS 5, which are in the larger ratios of n-butanol/water. This indicates that the complexing nature of urea selectively changes with change in the aqueous organic phase ratio. As reported in literature, the participation of extractant at the water – oil interface on metal ion extraction has been investigated experimentally and using atomic molecular dynamic (MD) simulations.[3] The MD simulations to investigate the role of urea in selective extraction of metal ions would give a better understanding on the reaction dynamics at interfaces. However, such investigation exceeds the scope of the current study but is the focus of future work.

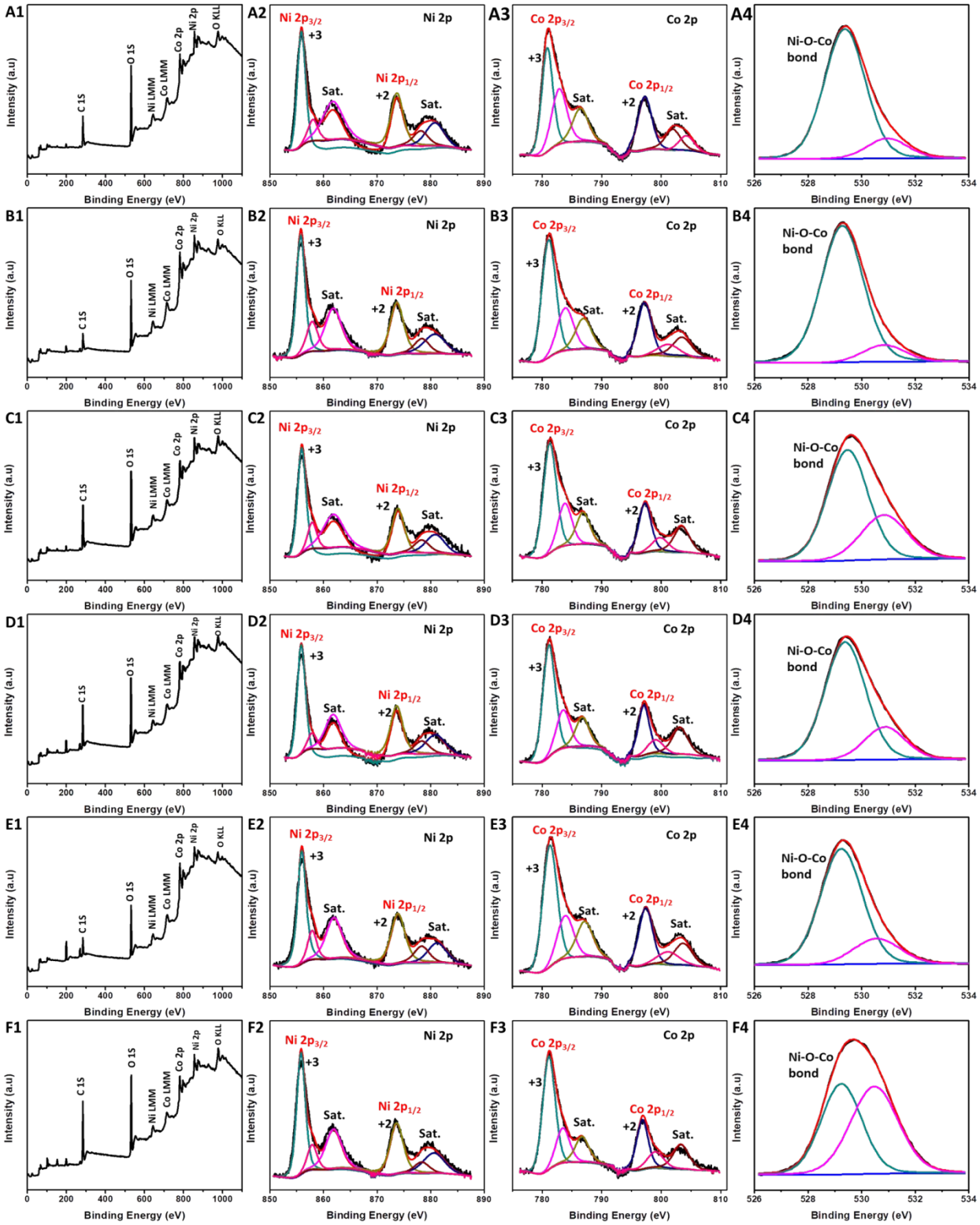

Figure S6. Deconvoluted XPS spectra of SS 1 (A1-A4), BS 1 (B1-B4), BS 2 (C1-C4), BS 4 (D1-D4), BS 5 (E1-E4) and SS 2 (F1-F4) samples.

The spectra show the presence of $2p_{1/2}$ and $2p_{3/2}$ states of both nickel and cobalt and metal-oxygen bond. The peaks around 856 eV and 874 eV corresponds to the +3 and +2 oxidation states of nickel

and the peaks around 781 eV and 797 eV corresponds to the +3 and +2 oxidation states of cobalt, respectively.[1,4] The rest of the marked peaks in the spectra correspond to the shakeup satellites.[4] In the case of oxygen, the peak at 529 eV corresponds to the metal – oxygen bond, and the other less intense peaks arise due to the presence of hydroxyl groups or large number of defect sites with low oxygen co-ordination in the samples.[1]

Sl No.	Electrode	Linear range (µM)	LOD (µM)	Reference
1	Pd-NP/RGO	1 - 150	0.233	S5
2	ERGO/Au	0.1 - 10	0.04	S6
3	p-GLY/GO	0.2 - 62	0.01	S7
4	ZnO NSB/GF	1 - 180	0.01	S8
5	SPCE/CQD	1 - 7	0.099	S9
6	GNP/PANI	3 - 115	0.8	S10
7	BS Flake	1 - 150	0.21	This work

Table S2. Comparison of the linear range and LOD of the BS Flake modified electrode with previously reported DA sensors.

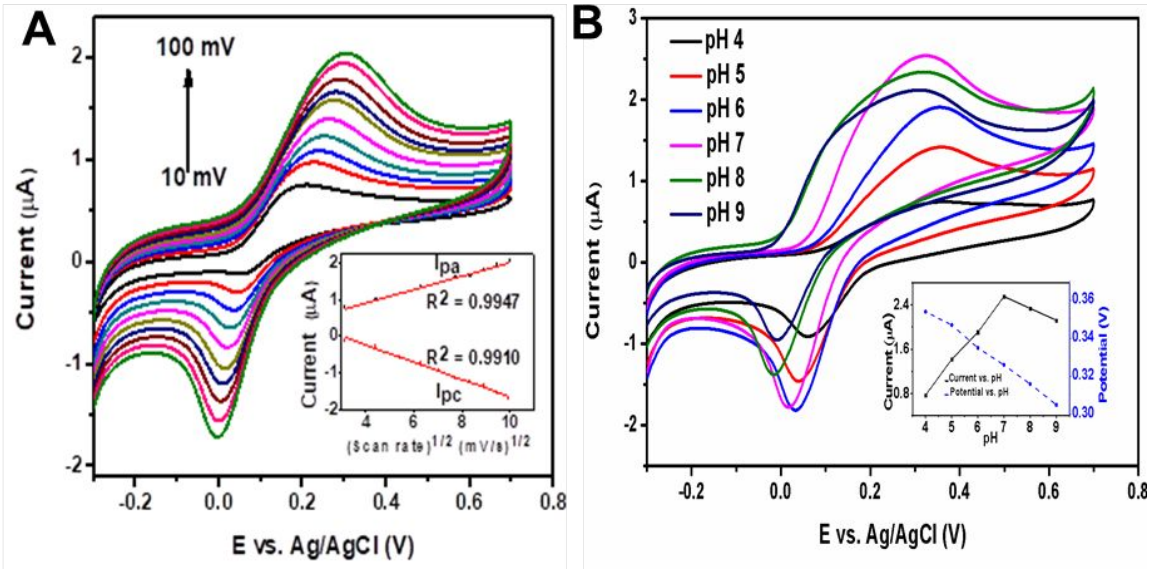

Figure S7. The effect of (A) pH and (B) scan rate on the detection of dopamine.

The effect of varying pH on the oxidation of DA has also been studied. It can be seen that the pH influences both the anodic peak current and the peak potential and hence serves as an important factor in the oxidation of DA. As seen in Figure, the increasing pH shifts the oxidation peak potential to lower values, confirming the involvement of the protons in the reaction.[11] In the case of anodic peak current, there is a successive increase in the peak current corresponding to an increase in pH from 4 to 7, followed by an eventual decrease. These results can be elucidated on the fact that lower pH generates more H^+ ions, which in turn act as a hindrance for the diffusion of more positively charged DA to the electrode surface resulting in a lower current and increased potential. However, the increased pH more than 7 can retard the reaction by facilitating several other cyclisation and polymerization reactions at the electrode surface.[12] Hence, owing to the better peak current and peak resolution, it can be concluded that pH 7.2 is the optimum pH for the detection of DA at nickel cobaltite modified electrodes, which very well matches with the body pH.

The impact of the scan rate on the peak current has also been examined. It is seen that both the anodic and cathodic peak currents increase consecutively with the scan rate from 10 mV to 100 mV. However, there is a slight shift in both the anodic and cathodic peak to positive and negative sides respectively, pointing to a quasireversible reaction.[13] Moreover, the increased peak separation on moving to higher scan rates can also be observed, which can be due to the thin layer effect.[14] An increased scan rate forbids the diffusion through the pores due to the inadequacy of sufficient time, thereby hindering the influence of thin layer. Thus, the oxidation occurs at a delayed potential, resulting in a greater peak separation.[15] Furthermore, the calibration curve of anodic and cathodic peak current *vs.* $(\text{scan rate})^{1/2}$ gives a linear plot with $R^2 = 0.9947$ and 0.9910 respectively, indicating a diffusion controlled redox reaction at the modified electrodes.[16,17]

REFERENCES

(1) Khalid, S.; Cao, C.; Wang, L.; Zhu, Y. Microwave Assisted Synthesis of Porous NiCo2O4 Microspheres: Application as High Performance Asymmetric and Symmetric Supercapacitors with Large Areal Capacitance. *Sci. Rep.* **2016**, *6*, 1–13.

(2) Fazlali, F.; Mahjoub, A. R.; Abazari, R. A New Route for Synthesis of Spherical NiO Nanoparticles via Emulsion Nano-Reactors with Enhanced Photocatalytic Activity. *Solid State Sci.* **2015**, *48*, 263–269.

(3) Qiao, B.; Muntean, J. V; Olvera, M.; Cruz, D.; Ellis, R. J. Ion Transport Mechanisms in Liquid-Liquid Interface. *Langmuir*. **2017**, *33*, 6135-6142.

(4) Guene, M.; Guèye, M. Structural Characterisation of Nickel - Cobalt Spinelrelated Oxides of NixCo3- XO4 (0 ≤ x ≤ 1 . 2) Prepared by Four Different Routes Using XRD , FTIR , UV-Vis-NIR and XPS. *Ghana J. Sci.* **2017**, *55*, 27 – 36.

(5) Palanisamy, S.; Ku, S.; Chen, S. M. Dopamine Sensor Based on a Glassy Carbon Electrode Modified with a Reduced Graphene Oxide and Palladium Nanoparticles Composite. *Microchim. Acta.* **2013**, *180* (11–12), 1037–1042.

(6) Li, S. J.; Deng, D. H.; Shi, Q.; Liu, S. R. Electrochemical Synthesis of a Graphene Sheet and Gold Nanoparticle-Based Nanocomposite, and Its Application to Amperometric Sensing of Dopamine. *Microchim. Acta.* **2012**, *177* (3–4), 325–331.

(7) He, S.; He, P.; Zhang, X.; Zhang, X.; Liu, K.; Jia, L.; Dong, F. Poly(Glycine)/Graphene Oxide Modified Glassy Carbon Electrode: Preparation, Characterization and Simultaneous Electrochemical Determination of Dopamine, Uric Acid, Guanine and Adenine. *Anal. Chim. Act.* **2018**, *1031*, 75–82.

(8) Huang, S.; Song, S.; Yue, H.; Gao, X.; Wang, B.; Guo, E. ZnO Nanosheet Balls Anchored onto Graphene Foam for Electrochemical Determination of Dopamine in the Presence of Uric Acid. *Sensors Actuators, B Chem.* **2018**, *277*, 381–387.

(9) Devi, N. R.; Kumar, T. H. V.; Sundramoorthy, A. K. Electrochemically Exfoliated Carbon Quantum Dots Modified Electrodes for Detection of Dopamine Neurotransmitter. *J. Electrochem. Soc.* **2018**, *165* (12), G3112–G3119.

(10) Wang, A. J.; Feng, J. J.; Li, Y. F.; Xi, J. L.; Dong, W. J. In-Situ Decorated Gold Nanoparticles on Polyaniline with Enhanced Electrocatalysis toward Dopamine. *Microchim. Acta.* **2010**, *171* (3), 431–436.

(11) Zhang, R.; Jin, G. Di; Chen, D.; Hu, X. Y. Simultaneous Electrochemical Determination of Dopamine, Ascorbic Acid and Uric Acid Using Poly(Acid Chrome Blue K) Modified Glassy Carbon Electrode. *Sensors Actuators, B Chem.* **2009**, *138* (1), 174–181.

(12) Wen, X. L.; Jia, Y. H.; Liu, Z. L. Micellar Effects on the Electrochemistry of Dopamine and Its Selective Detection in the Presence of Ascorbic Acid. *Talanta.* **1999**, *50* (5), 1027–1033.

(13) Babaei, A.; Taheri, A. R. Nafion/Ni(OH)2 Nanoparticles-Carbon Nanotube Composite Modified Glassy Carbon Electrode as a Sensor for Simultaneous Determination of Dopamine and Serotonin in the Presence of Ascorbic Acid. *Sensors Actuators, B Chem.* **2013**, *176*, 543–551.

(14) He, Q.; Liu, J.; Liu, X.; Li, G.; Chen, D.; Deng, P.; Liang, J. A Promising Sensing Platform toward Dopamine Using MnO2 Nanowires/Electro-Reduced Graphene Oxide Composites. *Electrochim. Acta.* **2019**, *296*, 683–692.

(15) Keeley, G. P.; Lyons, M. E. G. The Effects of Thin Layer Diffusion at Glassy Carbon Electrodes Modified with Porous Films of Single-Walled Carbon Nanotubes. *Int. J. Electrochem. Sci.* **2009**, *4* (6), 794–809.

(16) Wu, K.; Hu, S. Electrochemical Study and Selective Determination of Dopamine at a Multi-Wall Carbon Nanotube-Nafion Film Coated Glassy Carbon Electrode. *Microchim. Acta.* **2004**, *144* (1–3), 131–137.

(17) Mani, V.; Devasenathipathy, R.; Chen, S. M.; Kohilarani, K.; Ramachandran, R. A Sensitive Amperometric Sensor for the Determination of Dopamine at Graphene and Bismuth Nanocomposite Film Modified Electrode. *Int. J. Electrochem. Sci.* **2015**, *10* (2), 1199–1207.